CrossMark

SPECIAL ISSUE ARTICLE

Time-dependent flow velocity measurement using two-dimensional color Doppler flow imaging and evaluation by Hagen–Poiseuille equation

Bo Zhang[1] · Yuqing Sun[1] · Lianghua Xia[1] · Junyi Gu[1]

Abstract This paper aims to develop a technique to assess velocity flow profile and wall shear stress (WSS) spatial distribution across a vessel phantom representing an artery. Upon confirming the reliability of the technique, it was then used on a set of carotid arteries from a cohort of human subjects. We implemented color Doppler flow imaging (CDFI) for measurement of velocity profile in the artery cross section. Two dimensional instantaneous and time-dependent flow velocity and WSS vector fields were measured and their waveforms of peak velocities based on the technique were compared with WSS values generated by Hagen–Poiseuille equation. Seventy-five patients with intima-media thickening were prospectively enrolled and were divided into an IMT group. At the same time, another 75 healthy volunteers were enrolled as the control group. All the subjects were scanned and the DICOM files were imported into our in-house program. Next, we determine the velocity profile of carotid arteries in a set of 150 human subjects and compared them again. The peak velocities by the CDFI and Hagen–Poiseuille equation techniques were compared and statistically evaluated. The amounts of deviation for the two measured WSS profiles were performed and we demonstrated that they are not significantly different. At two different flow settings with peak flow velocity of 0.1, 0.5 ($\times 10^{-11}$) m/s, the obtained WSS were 0.021 ± 0.04, 0.038 ± 0.05 m/s, respectively. For the patient population study, the mean WSS value calculated by Hagen–Poiseuille equation was 2.98 ± 0.15 dyne/cm^2, while it was 2.31 ± 0.14 dyne/cm^2 by our CDFI analysis program. The difference was not statistically significant ($t = -1.057$, $P = 0.259$). Similar to the Hagen–Poiseuille equation, a negative linear correlation was also found between the calculated WSS and intima-media thickness ($P = 0.000$). Using CDFI analysis, we found that the WSS distribution at the middle of the proximal plaque shoulder was larger than the top of the shoulder. CDFI can assess the velocity and WSS profile accurately and efficiently and may be used for clinical diagnosis of cardiovascular conditions.

Keywords Velocity flow profile · Intima-media thickening · Color Doppler flow imaging · Hagen–Poiseuille equation

Introduction

Carotid atherosclerosis and advanced plaque rupture are the main contributors of ischemic strokes [1–3]. In-vitro and in vivo studies have shown that a low average level, but large gradients and high oscillation of wall shear stress (WSS) enhance intima-media thickening and carotid atherosclerosis [4–8]. In the past, the Hagen–Poiseuille equation is the most commonly-used calculation method for WSS assessment with reasonable accuracy [9–11]. This technique is limited as it is unable to assess the localized WSS, especially near the plaque for irregular vessel geometry. As such, the Hagen–Poiseuille equation is not feasible as a clinical method to obtain steady vessel diameter and blood velocity in order to assess the regional WSS surrounding plaque in vivo [12]. With the advancement of modern ultrasound technology such as color

Bo Zhang and Yuqing Sun have contributed equally to this study.

✉ Bo Zhang
zhangbodongfang@qq.com

1 Department of Ultrasound in Medicine, Shanghai East Hospital, Tongji University School of Medicine, No. 150 Jimo Rd, Shanghai 200120, China

Doppler flow imaging (CDFI) and contrast ultrasound, not just the mean WSS can be derived, but the hemodynamics flow distribution across the artery may be measured and visualized for clinical examination. This can give rise to modern modes of characterization of plaques and diagnosis of atherosclerosis.

Evidence increasingly suggests that localized high WSS may trigger the rupture of the fibrous cap of plaque. Studies have reported that the ruptures of vulnerable plaques are often observed at plaque shoulder, where the WSS was considered to be the highest [13–16]. Hence, the assessment of the hemodynamic parameters such as localized WSS change is critical because it is useful in predicting the plaque rupture position.

Among the existing medical imaging modalities, the Doppler ultrasound is the most preferred for non-invasive imaging and analysis of anatomical structure in the human body. It is widely used in clinics and hospitals with good visualization of the structures. In addition to the many other types of other measurement in the body, Doppler ultrasound may be used for blood flow velocity measurement especially in blood vessels. This may then be used to determine shear stress based on the shear rate multiplied by the blood viscosity [17].

Pulsed wave Doppler technique is an alternative ultrasound technique routinely used to determine one-dimensional (1D) pulsatile blood flow velocity [18, 19] effectively and has been in practice for decades. However, the imaging modality is limited by its angle dependence. There are several two dimensional (2D) blood flow velocity profiling ultrasound-based imaging modalities, including: ultrasonic speckle velocimetry [20], vector flow imaging using plane wave excitation [21], ultrasonic perpendicular velocimetry [22], ultrasonic particle image velocimetry or commonly known as Echo PIV [23, 24], and CDFI [25]. Then from the velocity profiles, the WSS on the arterial wall can be characterized [26, 27]. It is well known that pulsate blood resulting in oscillatory WSS affects the innermost intima vessel layer and endothelium resulting in plaque aggravation and atherosclerosis [28].

Other ultrasound techniques pertain to the contrast-enhanced ultrasound (CEUS), which is the application of ultrasound contrast medium to traditional medical sonography. Ultrasound contrast agents come in the form of microscale gas-filled bubbles that are coated with a special material to reflect ultrasound waves and allow the pick-up of signals depicting the fluid motional characteristics. We note that such agents may come in different sizes and structures. Clinically, contrast agents pertain to gas-filled bubbles that are immersed in the blood stream after being introduced intravenously in the human. Typical contrast agents suspended in deionized water (up to 1×10^3 bubbles/ml) are based on aqueous solution of air microbubbles created using an agitation mechanism [29]. The higher the bubble concentration, the higher is the accuracy of the flow measurements [30]. Due to the excellent degree of echogenicity by the contrast media to reflect ultrasound waves back to the signal detector, the contrast of vessel tissue and blood can be differentiated. The velocity of the blood can also be determined. This can allow us to gain an inside view of the blood stream noninvasively. The contrast agent backscatter creates a ultrasound sonogram with such high resolution that velocity of flow can be visualized and even quantified. Relying on this concept of imaging blood flow, contrast ultrasound is commonly used to quantitatively and qualitatively visualize blood streams in the cardiovascular system. In principle, contrast ultrasonography works because of the contrast-enhancing agents that resonate at a sufficiently high frequency to serve as ultrasonic reflectors in diagnostic ultrasound. We also note that in some cases, the micro-air bubbles immersed in the blood may wear off under the combined effects of excessive blood pressure and exposure to ultrasound energy acting on them.

To profile the WSS distribution of an artery, CDFI is used to assess localized velocity profile across various section of the artery and thereby determine the WSS along plaques in the artery [17]. Other methods involving the technique are able to clinically measure the mean WSS values in arterial blood flow and in arteries with irregular geometry effectively and efficiently [31, 32].

We evaluate feasibility of using CDFI to assess the WSS spatial distribution at the plaque. In order to ensure the correctness of the data, the medical imaging modality is applied to assess the association between low WSS and intima-media thickening CCA and we then compare the measured velocity profiles with those by contrast ultrasound.

Methods

Flow circulatory test rig and ultrasound imaging system

The flow circulatory test rig consists of the ultrasound system Philips IE33 system (Philips Medical Systems, Andover, MA, USA) and Toshiba SSA-790A system (Toshiba Medical Systems, Japan) equipped with a linear transducer (L14–5W/60, transmit frequency 10 MHz) for data acquisition. It is able to generate pulsatile flow through our vessel phantom (Fig. 1). Synthetic tissue was used to surround the vessel with radius 4 mm in order to simulate the common carotid artery embedded within the human tissue, and then it was immersed in degassed water to enhance ultrasound transmission. The flow in the vessel was then imaged by color Doppler and evaluated using Hagen–Poiseuille equation.

Fig. 1 Flow circulatory rig setup in our experiment. A pump is used to induce the working fluid to flow through the vessel phantom with a pulsatile flow. The fluid pressure was continuously recorded with a pressure sensor. Color Doppler flow images were acquired using the Philips Medical Systems
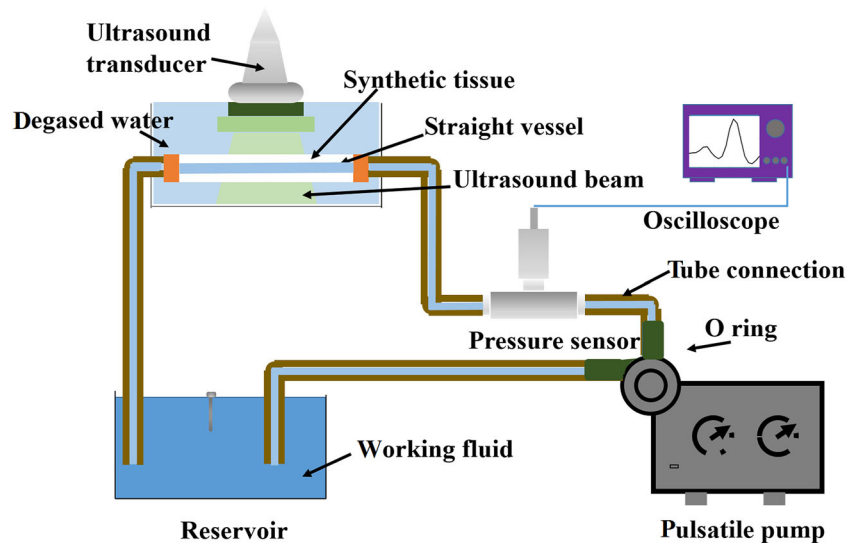
Velocity profile assessment using color Doppler flow imaging

High resolution imaging of arteries may be achieved by high frequency ultrasound within range of 10–12 MHz. Via nominal sound velocity of approximately 1540 m/s, the wavelength of sound transmitted into tissue by the high frequency sound wave can be obtained from the wave relationship, which implies that biological structures in the scale of this wavelength magnitude can be imaged accurately, i.e. up to 0.3 mm. Blood flow velocity profile can be measured accurately via the color Doppler effect. The principle works by reflecting ultrasound and detecting its frequency shift from the original source frequency. Such a frequency shift can be accurately obtained via the beat frequency between the incident and reflected sound waves, which is directly proportional to the velocity of flow. Therefore, continuous recording of the beat frequencies across a section of an artery generates the image of the time-dependent blood flow velocity profile (Fig. 2).

Wall shear stress assessment from CDFI

Based on Newtonian flow, the Hagen–Poiseuille equation determines the WSS simply by multiplying the gradient of velocity u_w at the artery wall with respect to the arterial radius r and the blood viscosity μ (Eq 1).

$$\tau_w = \mu \frac{u_w}{r}. \tag{1}$$

Our WSS mapping was designed on the basis of such a WSS definition equation by using the rate of change of velocity u with respect to r.

$$\tau_w = \mu \frac{du}{dr}\bigg|r = wall. \tag{2}$$

In this equation, τ_w refers to the WSS, μ is blood viscosity, $\frac{du}{dr}$ is velocity gradient (or shear rate), $r = wall$ is defined as r that is near the boundary of the artery. The CDFI in ultrasonic images was utilized to measure the spatial distribution of WSS. Because CDFI is able to indicate the level of blood flow velocity at each color pixel by an RGB value, the shear rate $\frac{du}{dr}$ can be calculated using Eq 3.

$$\tau_w = \mu \frac{V_{fast} - V_{slow}}{d}. \tag{3}$$

Here, V_{slow} is the velocity of the first blood flow pixel close to the vessel wall in the direction that is perpendicular to blood flow, and V_{fast} is the velocity of the second pixel. The dr in Eq. 2 is represented by d because the distance between the two adjacent pixels is constant. The velocity gradient at the vessel wall is calculated based on multiple values of V_{fast} and V_{slow}. Therefore, the shear rate could be calculated from the velocity profile by using Eq. 3. Shear stress can be obtained from shear rate calculated by multiplying blood viscosity, which was 3.0 cp in this study. The detailed algorithm has been presented in a previous report [17].

For our in-house program, three types of images can be designed to show the WSS distribution. They are two- and three- dimensional WSS maps, and also a fused WSS image. The two-dimensional WSS map is designed to quantitatively analyze the localized WSS at the vessel wall. The blue pixels indicate lower WSS values, while the red ones indicate the higher ones. The three-dimensional WSS map can be rotated freely to show the WSS distribution as it is a recommended procedure to observe the spatial distribution of blood shear stress directly via this technique. The fused WSS image illustrates the fusion of WSS dis-

Fig. 2 Blood velocity profiling based on color Doppler flow imaging. Based on the intensity modulated power spectrum, the beat frequency is correlated to the speed of the blood via frequency shift detection. Note that a considerable range of velocities may be present in the flow at any time based on a color *bar* scale from *red* to *blue*. Here, the *red* range of the color image pertains to a wide range of low velocities. The time-dependent velocity profile is expected to have a peak velocity value at the *center line* (*blue*) and dropping toward zero values at the walls (*red*)
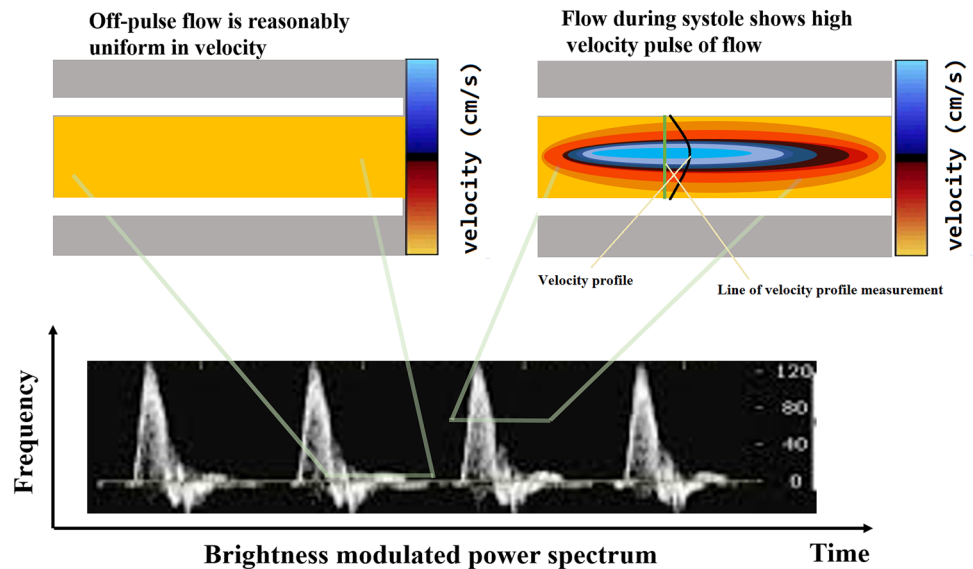
tribution and ultrasound image, and has been a suggested tool to observe the association between the vessel wall and WSS, thereby assisting physicians to analyze the association between IMT, plaque, blood velocity, vessel diameter and abnormal WSS in clinical practice.

Study population

The Ethics Committee of the Shanghai East Hospital approved the study. Written informed consent was obtained from all subjects. Seventy-five patients with intima-media thickening, abbreviated as IMT for (U/S detected: 0.9 mm < IMT ≤ 1.2 mm) were prospectively enrolled in the study (mean age 66.47 ± 13.47 years, range 46–83 years; 25 males) and were assigned as the IMT group. In addition, five patients with serious carotid artery plaques were enrolled (mean age 69.14 ± 6.23 years, range 58–79 years; 3 males). Also, another 75 healthy volunteers (U/S detected: IMT ≤ 0.9 mm) were enrolled (mean age 26.4 ± 3.47 years, range 19–32 years; 25 males) and assigned as the control group. None of the healthy volunteers had any history of cardiovascular disease, hypertension, diabetes or long-term smoking.

Experimental methods

Before the ultrasound examination, all subjects were allowed to rest in a supine position for 10 min. The subjects were studied in the supine position using a Philips IE33 system (Philips Medical Systems, Andover, MA, USA) and Toshiba SSA-790A system (Toshiba Medical Systems, Japan) by an experienced sonographer in our hospital. When scanning vessels in the longitudinal section, the scan depth was set just below the visualization of the

CCA. In the CDFI mode, the scale was adjusted to make the Doppler blood flow fill in the lumen without aliasing. Then, CDFI was acquired at the 2 cm below the CCA bifurcation in all subjects. For the five patients with plaque, CDFI was acquired near the plaque. Detailed ultrasound scanning methods were reported in the previous report [17]. Then, a smooth and uniform CDFI image was obtained. The DICOM files were imported into the program to perform WSS analyses and deliver graphic outputs such as three-dimensional WSS maps and fused WSS images.

Data analysis

All WSS data were analyzed by Microsoft Excel and SPSS 17.0 software (SPSS Inc., Chicago, IL, USA). The mean values of WSS distribution from the one hundred subjects were compared with the simulated results using a t test method. Correlation analyses were performed to explore the association between the intima-media thickness and WSS that were assessed by the CDFI and CFD for these subjects. We note that p value of less than 0.05 was considered statistically significant.

Results

Velocity and WSS distribution by color Doppler flow imaging

We developed a phantom model whereby the radius of the vessel is set at 0.001 m. All measurements were performed successfully and the simulated artery was studied in the transverse planes. The pressure profile and volumetric flow

rates were implemented as shown in Fig. 3. The CDFI DICOM images were then recorded. After importing the DICOM image, the WSS was assessed by Eq. (2). A typical example of the output is illustrated in Fig. 4. From the flow profile, we see that the red curve, which is based on the first measurement without averaging, has negligible

Fig. 3 Pressure and volume flow rate waveform profile used in our circulatory test rig. We implement a smaller and a larger peak at the pressure waveform to monitor a fluctuating velocity profile generated by them. This allows us to study if the color Doppler flow imaging can map the velocity waveform accurately
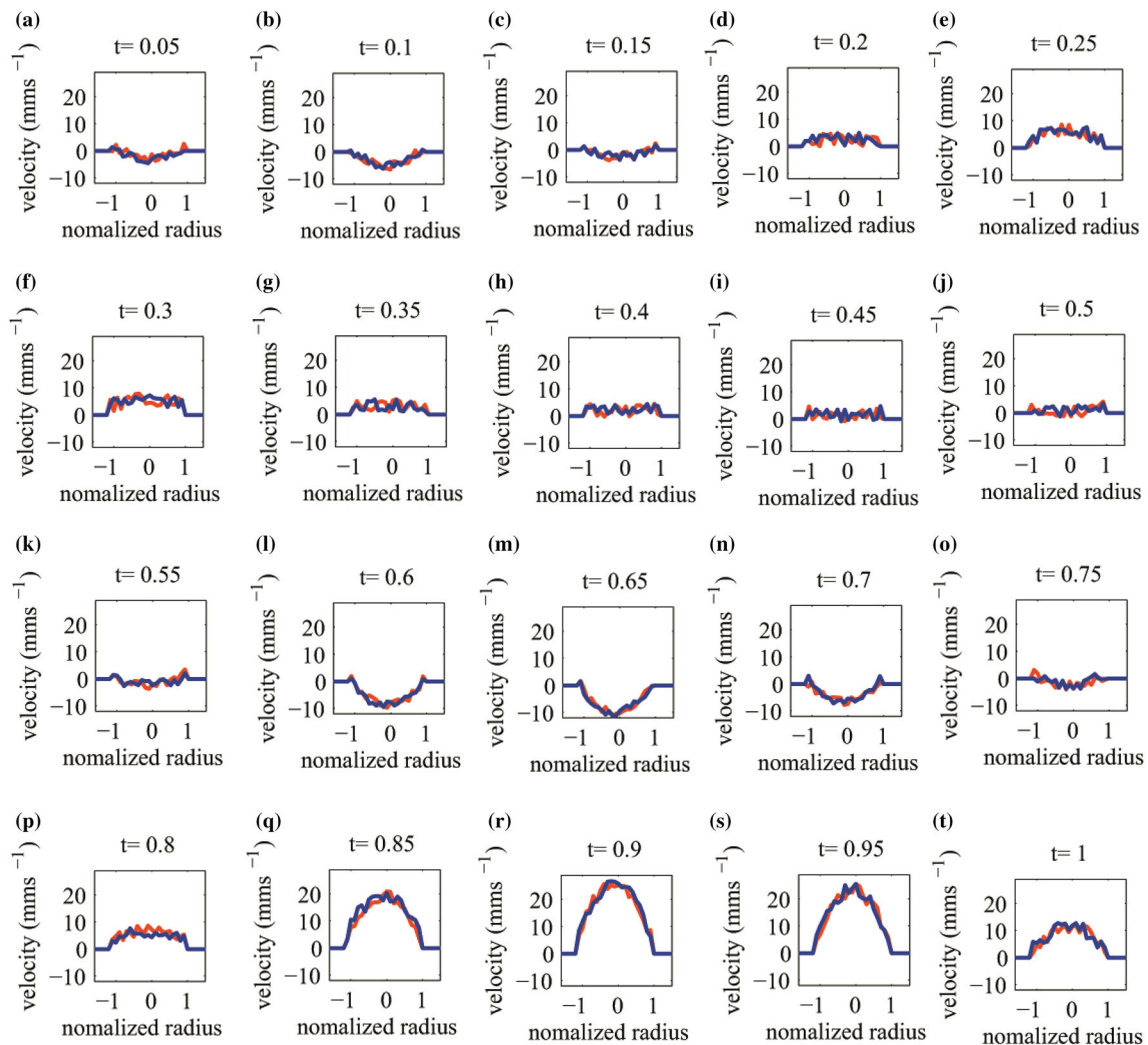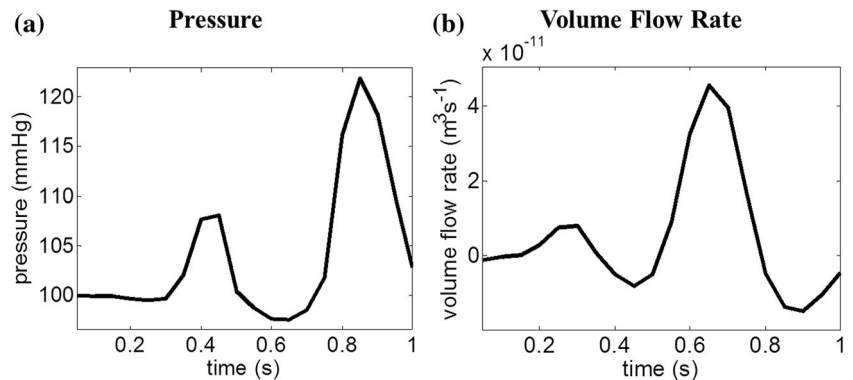

Fig. 4 Flow results computed by color Doppler flow imaging. The velocity flow profiles for time steps of 0.05–1.0, which were presented from (a) to (t), was derived from a set of flow images based on 20 trials of cyclic measurements at every same time step, which accounts for the irregular profile due to randomness during the pulsatile flow for every of the time step. The *red curve* represents the first measurement without averaging, whereas the blue curve represents the averaged results for all 20 trials
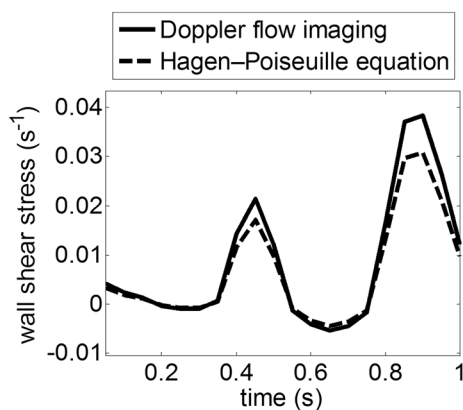
Fig. 5 Wall shear stress results comparison by Doppler flow imaging and Hagen–Poiseuille equation. The wall shear stress values can be determined from the velocity flow profiles imaged by Doppler ultrasound for one periodic cycle. The WSS that was derived from Hagen–Poiseuille equation under-predicts the true value

difference with the blue curve, which is based on averaging 20 trials of cyclic measurements at every same time step. Therefore since the fluctuations in values are not significant, we can use the flow measurement output at a particular time instance instead of averaging a series of measurements.

It is illustrated that the flow direction was changed as shown by the change in peak flow in the negative direction for $t = 0.05$–0.15 s in Fig. 4a–c, and from $t = 0.55$–0.75 s in Fig. 4k–o, and has been influenced by the reversal of flow caused by fluctuating pressure. Based on the velocity profile, we obtained the measured WSS values and produced the waveform as in Fig. 5.

The WSS derived from Hagen–Poiseuille equation deviates from the true value from the velocity profile that is imaged by both Doppler ultrasound methods as the linear approximation of the velocity gradient at the arterial wall tends to under-predict the real second-order degree of curvature of this gradient. There exists almost negligible difference between the CDFI and Hagen–Poiseuille equation techniques.

WSS assessment by color Doppler flow and evaluation using Hagen–Poiseuille equation

In order to evaluate the feasibility of the mean WSS value assessed by CDFI and Hagen–Poiseuille equation for irregular arterial geometries, the mean WSS values in intima-media thickening CCA in the IMT group were calculated by both methods and compared using an independent t test, which was shown in Fig. 6. We used dyne/cm^2 as the units for WSS in our paper, and we note that 1 dyne/cm^2 is the equivalent of 0.1 Pa in SI units.

Figure 6a showed that the mean WSS values in intima-media thickening CCA from both methods varies in the range 2–4 dyne/cm^2. The mean WSS value calculated by contrast ultrasound was 2.98 ± 0.15 dyne/cm^2, while it was 2.31 ± 0.14 dyne/cm^2 using our program. The difference between them was not statistically significant ($t = -1.057$, $P = 0.259$).

It has been widely known that WSS was negatively related to intima-media thickness. In our study, a negative linear correlation was also found between CDFI calculated WSS and intima-media thickness in our one hundred and fifty subjects ($r = -0.825$, $P = 0.000$, Fig. 6b). Meanwhile, the same correlation analysis was also performed using contrast ultrasound. It found that the negative liner correlation also exists between the WSS and intima-media thickness ($r = -0.813$, $P = 0.000$, Fig. 6c). It demonstrated that the WSS assessed by both ultrasound techniques can be applied to assess WSS and to evaluate the relationship of WSS and intima-media thickness as well.

Application of Doppler ultrasound in WSS assessment around plaque

The WSS assessment of a normal patient artery and a vessel with serious carotid artery plaques in a patient diagnosed with cardiovascular disease was generated from color Doppler ultrasound. Then, we implemented the CDFI method to verify this. The detailed flow profile was plotted at various cross-sectional planes of the artery (Fig. 7). In Fig. 7a, the pulsatile flow profile is seen to vary by observing the color intensity variation as measured by the color Doppler imaging for the normal healthy vessel. In Fig. 7b, we saw reduced blood flow peak velocities for the patients with serious plaque condition, which means a reduction in WSS for patients with intima-media thickening.

A representative fused image of the WSS regional distribution at the plaque shoulder was shown by Fig. 8 at a particular time step. It is well known that regions of low WSS followed by high oscillatory WSS influenced plaque growth significantly. In order to analyze the detailed WSS distribution at the plaque shoulder, two regions were set to analyze the WSS near the proximal plaque shoulder, which we defined as regions A and B. Interestingly, the two regions in the fused image were significantly different. The WSS distribution in region A was much brighter than that in region B. Data analysis showed that the mean WSS in region A was 13.67 dyne/cm^2 while it was 6.45 dyne/cm^2 in region B. It implies that the WSS values in region A were significantly larger than region B. However, the diameter (0.2 cm) and blood velocity (34 cm/s) in region A and B were similar. This new finding revealed by the

Fig. 6 The scatter diagram of mean WSS values and negative linear correlation were found between intima-media thickness (IMT) and WSS from color Doppler flow imaging. **a** These were values taken from our CDFI-based program and Hagen–Poiseuille equation in seventy-five patients with intima-media thickening CCA. The results show that the mean WSS values were similar for the two different methods. **b** WSS calculated by color Doppler, and the negative liner correlation was $r = -0.825$, $P = 0.000$; **c** WSS calculated by Hagen–Poiseuille equation, and the negative linear correlation was $r = -0.813$, $P = 0.000$
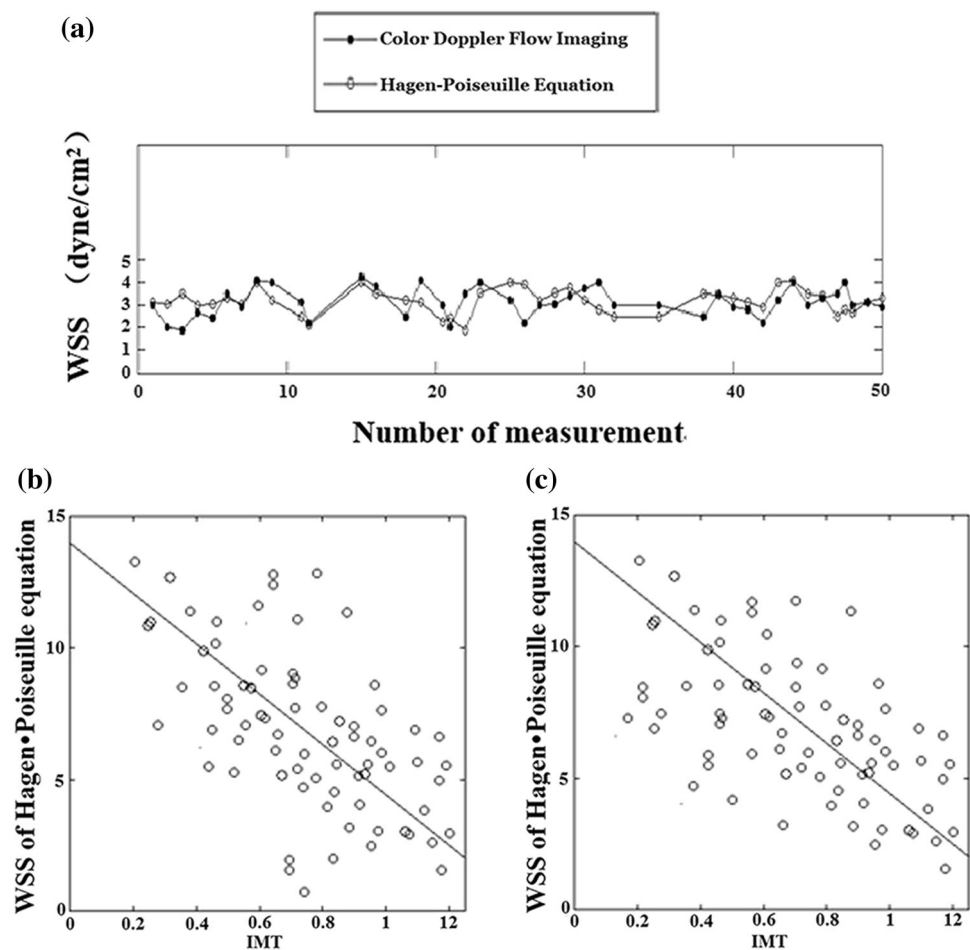
program implied the regional WSS distributions were vastly different even at the proximal plaque shoulder. The mechanism and reason was still unknown. It suggested more detailed regional WSS distribution analysis may be applied to surrounding plaque in order to predict the position of plaque ruptures.

Discussion

In our present study, CDFI has been introduced to explore the velocity and WSS distribution in carotid artery in vivo. The time-dependent cross-sectional flow velocity profiles from pulsatile flow velocity recordings can be obtained equally well with both the CDFI and Hagen–Poiseuille equation.

### Traditional WSS assessment in CCA

Previously, Hagen–Poiseuille equation is the most commonly performed WSS assessment method because the vessel diameter and the maximum flow velocity are easy to

obtain in vivo [33–35]. When the direction of blood flow is steady in intima-media thickening CCA, and the lumen is relatively coarse and uniform, the blood flow in intima-media thickening CCA approximates the Poiseuille flow. Therefore the WSS in intima-media thickening CCA that is calculated from the Hagen–Poiseuille equation is approximately accurate. It has been widely applied and many studies reported that the mean WSS values estimated by Hagen–Poiseuille equation are negatively correlated with the intima-media thickness [36, 37]. However, this technique fails for irregular geometries and computational fluid dynamics simulation can serve as an alternative to determining the WSS distribution instead.

The advantages of the Doppler-based methods

The CDFI can be used to construct the WSS distribution noninvasively based on a first order differential equation of velocity with respect to radial distance with good accuracy and feasibility [17]. Based on the velocities pertaining to CDFI blood pixels, we are able to calculate WSS, and plot the distribution for analysis.

Fig. 7 Color Doppler flow imaging of a normal and an atherosclerotic artery. Flow images of the arteries are shown at various time steps for (**a**) a normal artery, and (**b**) an artery that is stenosed. The peak velocity used to determine the WSS is measured at *green sectional line* of measurement upstream of the normal artery and then at another line of measurement at the stenosed region of the diseased artery
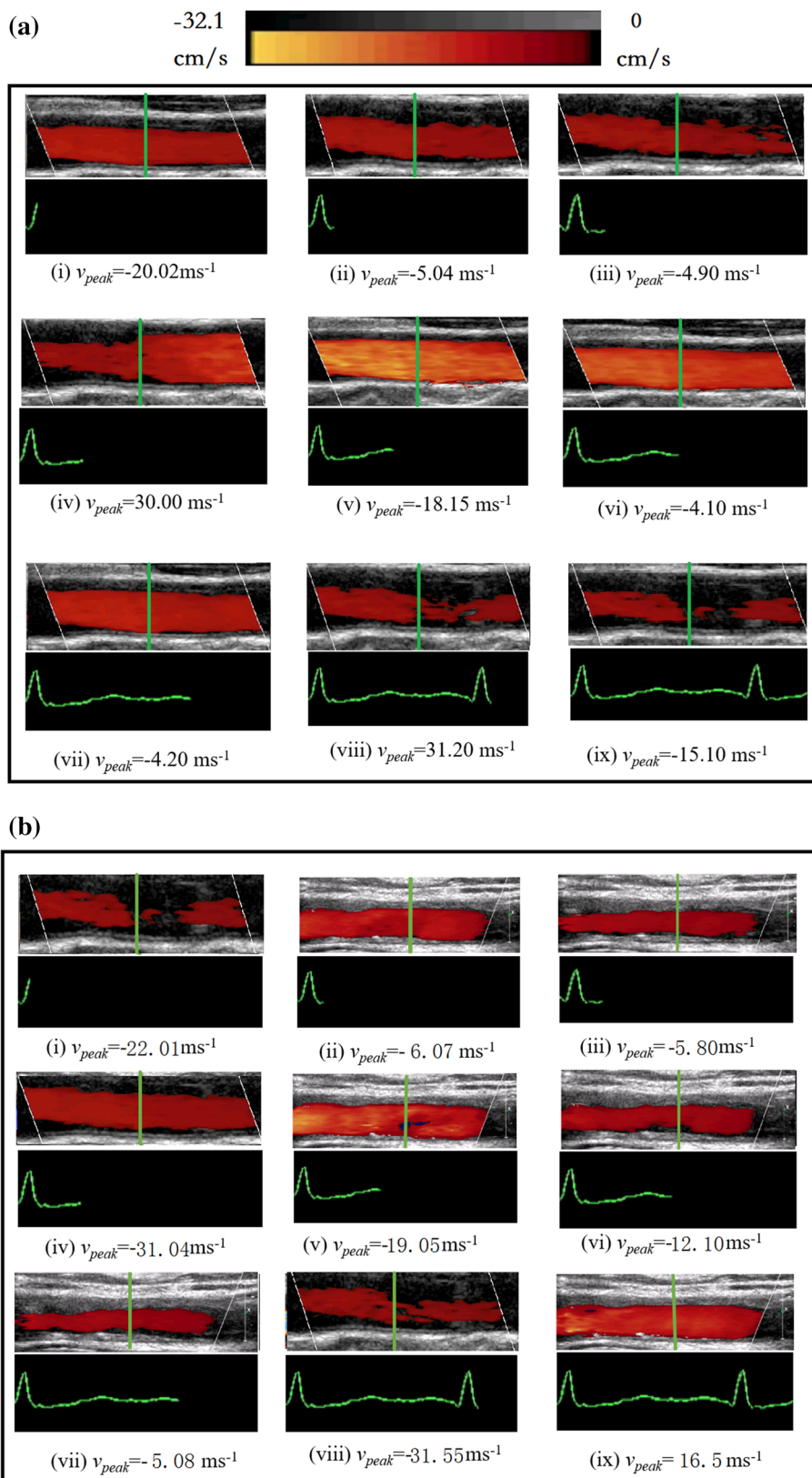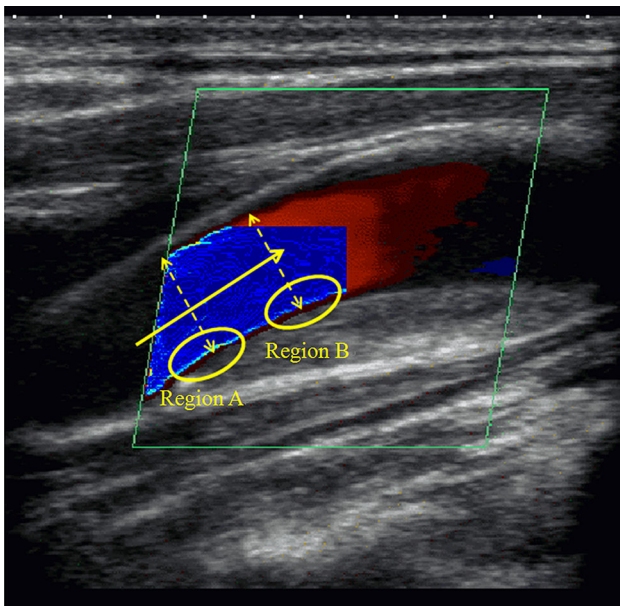
Fig. 8 A representative example of WSS regional distribution at plaque shoulder. Two regions were set to analyze the WSS near the proximal plaque shoulder which called *region A* and *region B*. The WSS values in *region A* were significantly larger than *region B*

In our study, the localized WSS distribution near the intima-media thickening carotid artery was displayed by a two-dimensional WSS map, a three-dimensional WSS map, and a fused image obtained from the program as shown in Fig. 9. The two-dimensional WSS map can be used for numerical analysis because it removed all factors unrelated to the shear stress distribution. It can analyze localized WSS quantitatively, which was more realistic and accurate due to the precise quantitative analysis calculated between each pixel. The three-dimensional WSS map can be rotated 360° for good visualization of the data landscape. It provided a more intuitive method to observe the spatial distribution of shear stress values. In this study, the three-dimensional WSS map shows that the anterior and posterior WSS distribution at intima-media thickening CCA is not the same although the algorithm is the same for every pixel. It implied that when change of velocity and lumen diameter was small, the variation of WSS near the intima-media thickening CCA still exists. Once the increased or decreased abnormal WSS is found, the three-dimensional WSS map can sensitively display the location coordinates for observation. The fused image combines the advantage of an ultrasound image together with shear stress distribution. It can be used to observe the lumen diameter, intima-media thickness and changes of vessel geometry at different abnormal WSS regions. It is a convenient tool to observe the relation between the localized WSS distribution and corresponding intima-media membrane and lumen diameter. In this study, Fig. 9a shows the fused WSS image

at the intima-media thickening region. Two bright bands, which were WSS spatial distribution, can be found (as marked by arrows in Fig. 9b) at the anterior and posterior wall in CCA. Compared with the healthy WSS at CCA, the brightness of WSS distribution at intima-media thickening portion was darker, and the width was narrowed and uniform. It suggests that the WSS values at the intima-media thickness portion were lower than the normal range. The WSS spatial distribution obtained by fused images can display local WSS changes at different locations accurately (Fig. 9c, d). This fused image is able to help physicians to observe the WSS distribution and its relationship with vessel walls intuitively. The situation such that WSS cannot be visualized by the Hagen–Poiseuille equation may now be reversed because of our CDFI program. In addition, our program can help researchers to quantitatively analyze the regional WSS values at intima-media thickening portions. Compared with the Hagen–Poiseuille equation, it can be used to observe detailed WSS values at localized positions. In our study, Fig. 6 shows that around 90 % of WSS varied between 2 and 6 dyne/cm^2, and the other 10 % of WSS varied between 6 and 8 dyne/cm^2. Furthermore, it found that most WSS values were among 2–4 dyne/cm^2. With the value increasing, the number of pixels decreased dramatically. The speed of the decrease was faster than a normal vessel. It implies that compared with the normal WSS at CCA, the variation of WSS near the intima-media thickness portion was lower, but high WSS values can also be found at intima-media thickness portions.

Accuracy evaluation of our CDFI-based program

In order to evaluate the correctness of our CDFI-based program that calculated the WSS in intima-media thickening CCA, the mean value was compared to the result calculated by the Hagen–Poiseuille equation. In this study, it showed that the difference between the mean WSS values from the program and the Hagen–Poiseuille approach were not statistically significant ($t = -0.864$, $p = 0.604$). In addition, negative linear correlations were found between WSS values and intima-media thickness by the two methods. It suggests that the mean WSS value calculated from the program is also feasible to assess the association between WSS and intima-media thickness just like Hagen–Poiseuille approach.

Regional WSS distribution surrounding plaque shoulder

CDFI can be utilized to profile flow velocity in the arteries. Flow in a region of obstruction results in a higher velocity peak to maintain the flowrate, and therefore, velocity
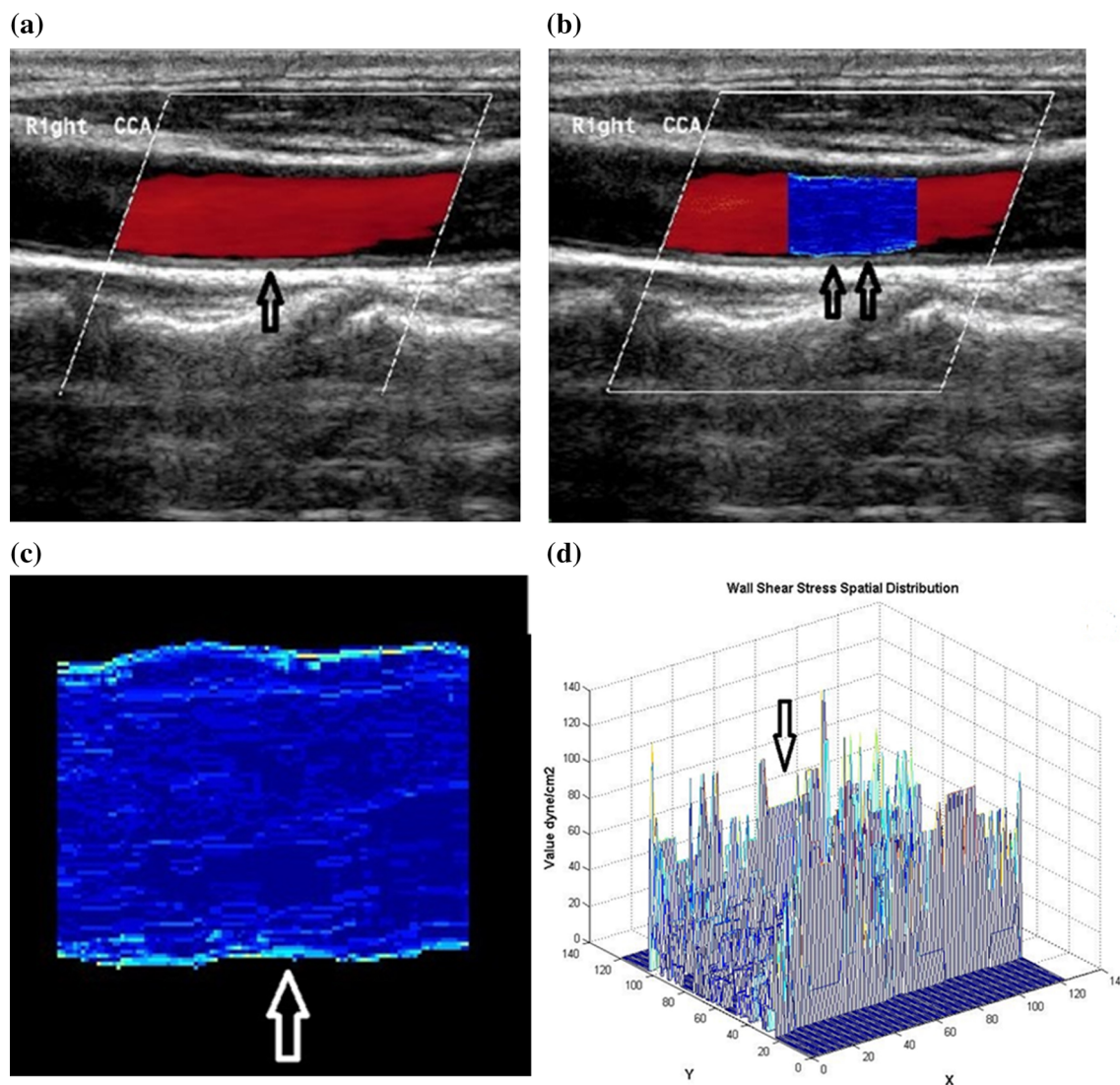
Fig. 9 Wall shear stress spatial distribution in intima-media thickening carotid artery generated by color Doppler flow imaging. **a** CDFI of intima-media thickening carotid artery; **b** the fused image of WSS spatial distribution, which was a convenient tool to observe the relation between the localized WSS distribution and corresponding intima-media membrane and lumen diameter; **c** two-dimensional distribution of WSS in the intima-media thickening carotid artery, which can analyze localized WSS quantitatively; and **d** Three-dimensional distribution of WSS intima-media thickening carotid artery, which provided a more intuitive method to observe the spatial distribution of shear stress

profiling of arteries can be used to detect narrowing of the vessel.

Although it has been well-accepted that atherosclerosis initiation and early progression correlate negatively with WSS, increasing evidence suggests that when lesions continue to grow and eventually intrude into the lumen and form plaque, the WSS surrounding it increases substantially. Some studies have demonstrated that high shear stress may be related to plaque rupture [38–40]. It is hoped that the research on assessing this WSS distribution near the plaque will accurately discover plaque rupture positions. Unfortunately, in vivo evidence of such a relation is limited because the Hagen–Poiseuille equation cannot be applied to assess WSS near plaque as the geometry of vessels with plaque is irregular and the blood flow direction may change. However, the flow velocity gradient near the plaque remains relatively constant. Hence, the program can measure the WSS near plaque sensitively, which we aim to introduce it as one of the well-established methods for estimating the WSS near plaques in vivo.

In our study, the WSS values near the plaque shoulder do not decrease. On the contrary, they increased significantly. The WSS values at regions A and B of the proximal plaque shoulder were significantly higher than the normal

WSS range. It demonstrated that the WSS values near carotid plaque were larger than those at normal carotid arteries, which may explain why the plaque usually ruptures at plaque shoulders. Moreover, the WSS values at region A were significantly greater than those at region B. One possible reason was that the vessel wall at region A directly withstands the impact of high speed blood flow, resulting in most of the direction change of blood flow occurring around them. Hence the friction there becomes greater than the other regions of the plaque. Some studies have reported the association between increased WSS at the plaque shoulder and plaque ruptures. Dirksen et al. [41] reported that the WSS near the plaque was associated with the plaque ruptures. Plaque ruptures always occur at the shoulder of plaque, where the WSS was larger than normal value range. Slager et al. [42] reported that local biologic effects induced by high shear stress can destabilize the cap and turn it into a rupture-prone vulnerable plaque. Groen et al. [43] found that the ruptures of vulnerable plaques are often observed at the upstream region of the plaque, where the WSS is considered to be highest. Fukumoto et al. [31] proposed that localized high shear stress may be a trigger of fibrous cap ruptures.

Limitations and future developments

The observed WSS distribution can only represent WSS for longitudinal vessels. The WSS data from CDFI are not three-dimensional data as compared to magnetic resonance imaging. However, ultrasound scanning is simple, time-saving and relatively economical compared with nuclear imaging, which makes WSS assessment easier to apply. In addition, our CDFI-based program cannot be applied for the WSS detection of the coronary artery because coronary blood vessels cannot be observed by regular ultrasound. Fortunately, the research of WSS assessment by angiography, and intravascular ultrasound make up this limitation.

Our study found that the WSS values are different for different regions of plaque shoulders. However until now, there have been no serial studies to find the accurate position of plaque ruptures. The in vivo relationship between WSS and plaque ruptures remains unclear. The approximate WSS estimation is not sufficient to explore the position of fibrous cap destruction. Therefore, our group plans to increase the volume of patients with plaque in a follow-up study. Plaques are planned to be divided into the following five regions: bottom of proximal plaque, the shoulder of proximal plaque, the top of plaque, the shoulder of distal plaque and the bottom of distal plaque, in order to further observe the distribution of WSS at different regions. Then, patients were followed up and the position of plaque rupture will be recorded to explore the association between plaque ruptures and increased WSS aiming at providing valuable references for predicting the location of plaque ruptures.

Conclusions

This study demonstrated that color Doppler flow can be utilized to assess the velocity profile of blood flow in carotid arteries and predict WSS near plaque shoulders. Moreover, the spatial WSS distribution makes the WSS visualization easier, which could accurately and quickly observe the localized WSS modifications. Since CDFI is easy to obtain during routine ultrasound scanning, we can harness ultrasound to be able to serve as a convenient tool to predict the position of plaque rupture in clinical practice.

References

1. Niu L, Zhang Y, Meng L et al (2014) Detection of subclinical atherosclerosis in asymptomatic subjects using ultrasound radiofrequency-tracking technology. PLoS One 9:e111926
2. Liu M-E, Liao Y-C, Lin R-T et al (2013) A functional polymorphism of PON1 interferes with microRNA binding to increase the risk of ischemic stroke and carotid atherosclerosis. Atherosclerosis 228:161–167
3. Molnar T, Pusch G, Papp V et al (2014) The L-arginine pathway in acute ischemic stroke and severe carotid stenosis: temporal profiles and association with biomarkers and outcome. J Stroke Cerebrovasc Dis 23:2206–2214
4. Niu L, Qian M, Yang W et al (2013) Surface roughness detection of arteries via texture analysis of ultrasound images for early diagnosis of atherosclerosis. PLoS One 8:e76880
5. Qian M, Niu L, Wong K, Abbott D, Zhou Q, Zheng H (2014) Pulsatile flow characterization in a vessel phantom with elastic wall using ultrasonic particle image velocimetry technique: the impact of vessel stiffness on flow dynamics. Biom Eng IEEE Trans 61(9):2444–2450
6. Galizia MS, Barker A, Liao Y et al (2014) Wall morphology, blood flow and wall shear stress: MR findings in patients with peripheral artery disease. Eur Radiol 24:850–856
7. Tripolino C, Irace C, Scavelli FB et al (2014) Triglyceride glucose index and common carotid wall shear stress. J Investig Med 62:340–344
8. Peiffer V, Sherwin SJ, Weinberg PD (2013) Does low and oscillatory wall shear stress correlate spatially with early atherosclerosis? A systematic review. Cardiovasc Res, cvt044
9. Gopalakrishnan SS, Pier B, Biesheuvel A (2014) Global stability analysis of flow through a fusiform aneurysm: steady flows. J Fluid Mech 752:90–106
10. Owolabi MO, Agunloye AM, Ogunniyi A (2014) The relationship of flow velocities to vessel diameters differs between extracranial carotid and vertebral arteries of stroke patients. J Clin Ultrasound 42:16–23

11. Mynard JP, Wasserman BA, Steinman DA (2013) Errors in the estimation of wall shear stress by maximum Doppler velocity. Atherosclerosis 227:259–266

12. Towne JB, Quinn K, Salles-Cunha S, Bernhard VM, Clowry LJ (1982) Effect of increased arterial blood flow on localization and progression of atherosclerosis. Arch Surg 117:1469–1474

13. Nigro P, Abe J-I, Berk BC (2011) Flow shear stress and atherosclerosis: a matter of site specificity. Antioxid Redox Signal 15:1405–1414

14. Corban MT, Eshtehardi P, Suo J et al (2014) Combination of plaque burden, wall shear stress, and plaque phenotype has incremental value for prediction of coronary atherosclerotic plaque progression and vulnerability. Atherosclerosis 232:271–276

15. Silva Marques J, Pinto FJ (2014) The vulnerable plaque: current concepts and future perspectives on coronary morphology, composition and wall stress imaging. Port J Cardiol 33:101–110

16. Assemat P, Armitage JA, Siu KK et al (2014) Three-dimensional numerical simulation of blood flow in mouse aortic arch around atherosclerotic plaques. Appl Math Model 38:4175–4185

17. Wang C, Chen M, Liu S-L, Liu Y, Jin J-M, Zhang Y-H (2013) Spatial distribution of wall shear stress in common carotid artery by color doppler flow imaging. J Digit Imaging 26:466–471

18. Aaslid R, Markwalder T-M, Nornes H (1982) Noninvasive transcranial Doppler ultrasound recording of flow velocity in basal cerebral arteries. J Neurosurg 57:769–774

19. Overbeck JR, Beach KW, Strandness DE (1992) Vector Doppler: accurate measurement of blood velocity in two dimensions. Ultrasound Med Biol 18:19–31

20. Sandrin L, Manneville S, Fink M (2001) Ultrafast two-dimensional ultrasonic speckle velocimetry: a tool in flow imaging. Appl Phys Lett 78:1155–1157

21. Udesen J, Gran F, Hansen K, Jensen JA, Thomsen C, Nielsen MB (2008) High frame-rate blood vector velocity imaging using plane waves: simulations and preliminary experiments. IEEE Trans Ultrason Ferroelectr Freq Control 55:1729–1743

22. Beulen B, Verkaik AC, Bijnens N, Rutten M, van de Vosse F (2010) Perpendicular ultrasound velocity measurement by 2D cross correlation of RF data. Part B: volume flow estimation in curved vessels. Exp Fluids 49:1219–1229

23. Zhang F, Lanning C, Mazzaro L, Barker AJ, Gates PE, Strain WD, Fulford J, Gosling OE, Shore AC, Bellenger NG (2011) In vitro and preliminary in vivo validation of echo particle image velocimetry in carotid vascular imaging. Ultrasound Med Biol 37:450–464

24. Zheng H, Liu L, Williams L, Hertzberg JR, Lanning C, Shandas R (2006) Real time multicomponent echo particle image velocimetry technique for opaque flow imaging. Appl Phys Lett 88:261915

25. Merritt CR (1987) Doppler color flow imaging. J Clin Ultrasound 15(9):591–597

26. Humphrey JD (2008) Mechanisms of arterial remodeling in hypertension coupled roles of wall shear and intramural stress. Hypertension 52:195–200

27. Qiu Y, Tarbell JM (2000) Interaction between wall shear stress and circumferential strain affects endothelial cell biochemical production. J Vasc Res 37:147–157

28. Li Y-SJ, Haga JH, Chien S (2005) Molecular basis of the effects of shear stress on vascular endothelial cells. J Biomech 38:1949–1971

29. Qian M, Niu L, Wang Y, Jiang B, Jin Q, Jiang C, Zheng H (2010) Measurement of flow velocity fields in small vessel-mimic phantoms and vessels of small animals using micro ultrasonic particle image velocimetry (micro-EPIV). Phys Med Biol 55:6069

30. Niu L, Qian M, Wan K, Yu W, Jin Q, Ling T, Gao S, Zheng H (2010) Ultrasonic particle image velocimetry for improved flow gradient imaging: algorithms, methodology and validation. Phys Med Biol 55:2103

31. Fukumoto Y, Hiro T, Fujii T et al (2008) Localized elevation of shear stress is related to coronary plaque rupture: a 3-dimensional intravascular ultrasound study with in vivo color mapping of shear stress distribution. J Am Coll Cardiol 51:645–650

32. Evans DH, Jensen JA, Nielsen MB (2011) Ultrasonic colour Doppler imaging. Interface Focus 1:490–502

33. Reneman RS, Vink H, Hoeks AP (2009) Wall shear stress revisited. Artery Res 3:73–78

34. Wong K, Mazumdar J, Pincombe B, Worthley SG, Sanders P, Abbott D (2006) Theoretical modeling of micro-scale biological phenomena in human coronary arteries. Med Biol Eng Comput 44:971–982

35. Wu J, Liu G, Huang W, Ghista DN, Wong KK (2014) Transient blood flow in elastic coronary arteries with varying degrees of stenosis and dilatations: CFD modelling and parametric study. Comput Methods Biomech Biomed Eng 18:1–11

36. Efstathopoulos EP, Patatoukas G, Pantos I, Benekos O, Katritsis D, Kelekis NL (2008) Measurement of systolic and diastolic arterial wall shear stress in the ascending aorta. Phys Med 24:196–203

37. Wong KK, Thavornpattanapong P, Cheung SC, Tu J (2013) Numerical stability of partitioned approach in fluid-structure interaction for a deformable thin-walled vessel. Comput Math Methods Med

38. Papafaklis MI, Koskinas KC, Chatzizisis YS, Stone PH, Feldman CL (2010) In-vivo assessment of the natural history of coronary atherosclerosis: vascular remodeling and endothelial shear stress determine the complexity of atherosclerotic disease progression. Curr Opin Cardiol 25:627–638

39. Wellnhofer E, Goubergrits L, Kertzscher U, Affeld K, Fleck E (2009) Novel non-dimensional approach to comparison of wall shear stress distributions in coronary arteries of different groups of patients. Atherosclerosis 202:483–490

40. Yang C, Canton G, Yuan C, Ferguson M, Hatsukami TS, Tang D (2010) Advanced human carotid plaque progression correlates positively with flow shear stress using follow-up scan data: an in vivo MRI multi-patient 3D FSI study. J Biomech 43:2530–2538

41. Dirksen MT, van der Wal AC, van den Berg FM, van der Loos CM, Becker AE (1998) Distribution of inflammatory cells in atherosclerotic plaques relates to the direction of flow. Circulation 98:2000–2003

42. Slager C, Wentzel J, Gijsen F et al (2005) The role of shear stress in the destabilization of vulnerable plaques and related therapeutic implications. Nat Clin Pract Cardiovasc Med 2:456–464

43. Groen HC, Gijsen FJ, van der Lugt A et al (2007) Plaque rupture in the carotid artery is localized at the high shear stress region a case report. Stroke 38:2379–2381